

Some preliminary results on the influence of riblets on the structure of a turbulent boundary layer

A. Baron and M. Quadrio

Dipartimento di Ingegneria Aerospaziale del Politecnico di Milano, Milano, Italy

A comparison of hot-wire measurements over flat and ribletted walls is described. Details of the experimental apparatus and procedures are given, together with some preliminary results. The test is validated by the calculation of the parameters of the boundary layer, by the comparison of the usual profiles of the streamwise component of the velocity with the available experimental data, and by a conditional analysis of the instantaneous signal. Mean and rms profiles for the streamwise component of the velocity evidence, for the riblet plate, an upward shift in law-of-the-wall plots and an overall, small reduction in fluctuation intensities across the boundary layer. Skewness and flatness factors appear to be unchanged. Time series of velocity samples are analyzed by means of power spectra, correlations, and conditional techniques. In particular, the VITA technique, used as an ejection detector, gives results in agreement with previous studies for the flat-plate case, and suggests a moderate increase of the ejection frequency over the riblet surface. Accordingly, the time/space scales of the events appear to be shorter for the riblet-plate flow.

Keywords: turbulence; riblets; drag reduction; conditional sampling

Introduction

In the last 15 years, turbulent drag reduction by passive means has become an important task in industrial development. Passive techniques like the use of riblets are particularly attractive because of their simplicity, even if their benefit is of the order of some percent (up to 7–8 percent) in terms of skin-friction reduction. The reader is referred to the recent work of Walsh (1990) for an exhaustive review on riblets.

Geometrical characteristics and operating conditions necessary to obtain maximum performance are now reasonably assessed, due to the large amount of experimental work carried out on turbulent boundary layers and channel flows over ribletted surfaces (see, for example, Walsh 1982; Vukoslavcevic et al. 1987; Liu et al. 1990; Coustols and Cousteix 1990). While numerical research still presents several problems related to the difficulty of simulating turbulent flows in complex geometries, so that direct numerical simulation appears to be still unpractical (Rogallo and Moin 1984), a number of water-channel and wind-tunnel tests are available in the literature. Most of them deal with global measurements of the effects of riblets on the boundary layer, but some (e.g., Vukoslavcevic et al. 1987) are concerned with the analysis of the flow field in the vicinity of and inside the grooves. Such complex experiments have used particular instrumentation (tunnels with very large turbulent length scales; laser-Doppler anemometry; very small hot wires); they have supplied data for understanding the actual modifications induced by riblets, for example, in the spanwise distribution of the *local* friction coefficient, and have confirmed

the hypothesis that one of the main mechanisms by which riblets are effective is purely viscous—they are able to counterbalance the increase in wetted surface. This hypothesis is also supported by numerical studies of Djenidi et al., who excluded the possibility of drag increase in laminar riblet flow.

Nevertheless, to date it is still questionable how riblets do actually work in reducing friction drag, and there is no general agreement between researchers even about the influence of riblets on some characteristics of the flow when comparing flat and ribletted surfaces (Walsh 1990).

On the other hand, in recent years numerical tools have become more and more important in the understanding of the complex flow dynamics in the near wall region of turbulent boundary layers. Huge databases are now available from highly accurate direct numerical simulation of turbulent flows, and their analysis (Johansson, Alfredsson, and Kim 1991) gave the opportunity of highlighting several problems encountered in the application of conditional averaging techniques to the raw experimental data. As a consequence, and especially for the flat-plate case, conditional techniques are now one of the most powerful tools for extracting quantitative information on turbulence.

The objective of the present work is, first of all, to present an accurate and repeatable experimental comparison of the characteristics of turbulent boundary layers over flat and ribletted surfaces, mainly based on hot-wire anemometry, so as to contribute to the clarification of the still open problems in this area (e.g., the extent to which the riblet effect is felt in the boundary layer, or the determination of the ejection frequency). Secondly, a preliminary analysis of the hot-wire instantaneous data is presented, in order to verify the quality of the test even in terms of the instantaneous velocity signal by comparing conditionally sampled data with results available in the literature. This analysis also allows us to draw some conclusions about the way in which riblets affect the whole

Address reprint requests to Professor Baron at Dipartimento di Ingegneria Aerospaziale del Politecnico di Milano, via C. Golgi 33, 20133 Milano, Italy.

Received 22 April 1992; accepted 18 November 1992

bursting cycle. Development and tests of more refined techniques of conditional analysis are currently in progress.

Equipment

Experiments are performed in the L7⁺ Low Speed Wind Tunnel at the Von Kármán Institute for Fluid Dynamics (Bruxelles), operated so as to obtain a thick boundary layer with large scales of turbulence. L7⁺ is an open-return wind tunnel with a speed range from 0 to 20 m/s. The flow field is established by a 0.32-m-diameter 43-blade radial fan powered by a 1-hp variable-speed a.c. motor. Downstream of the fan, the flow expands through a diffuser until the cross-sectional flow area is 0.81 m × 1.08 m. Boundary-layer separation in the diffuser is avoided by using three fine-mesh screens. The settling chamber downstream of the diffuser is 0.74 m long before the flow enters the contraction into the test section.

The test section (Figure 1) is 1700 mm long, 300 mm wide, and 93 mm high. These dimensions are believed not to allow an exhaustive analysis of the scaling of quantities like the ejection frequency with the Reynolds number (Shah and Antonia 1989), but to be sufficient for the comparison of two different flows at nominally the same Reynolds number. The upper wall of the test section is adjusted in order to obtain a nominally zero pressure gradient. A turbulent boundary layer is generated by means of a trip strip located 50 mm downstream the leading part of the test section. The leading and trailing parts of the lower wall of the test section remain unchanged, while its intermediate section (770 mm long) can be removed and replaced with flat or ribletted plates. In the present experiment the ribletted surface, in brass, has machined into its central part (200 mm wide) small streamwise triangular grooves, of height $h = 0.7$ mm and spacing $s = 0.7$ mm. These dimensions, normalized by the viscous length scale, are

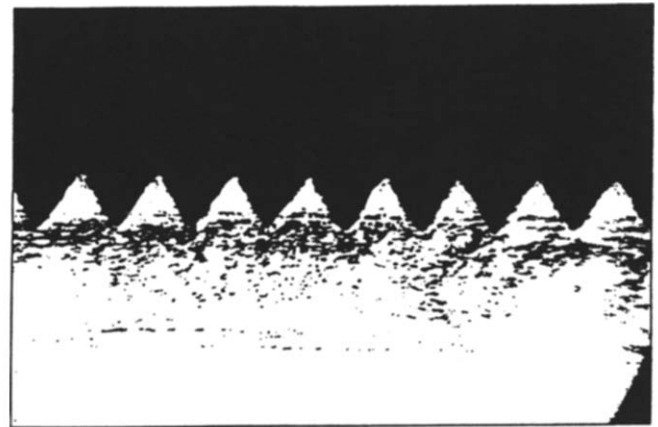


Figure 2 Microphotograph of riblet contour

equivalent to $s^+ = 12$ and $h^+ = 12$ wall units, i.e., they correspond to the range of optimum performance of the riblets. The riblet plate is mounted with peaks flush with the leading flat surface; the layout with riblet valleys flush with the flat plate has been proved (Lazos and Wilkinson 1988) to have no influence on the performances of the riblets. The cross-sectional shape, which is known (Walsh and Lindemann 1984) to have a first-order effect on the amount of drag reduction, is realized with maximum care. Figure 2 shows a microphotograph of the actual shape of the riblet contour. A quantitative evaluation of the manufacturing process and of the actual shape is given in Section 4.

A single hot-wire probe is used that has length and diameter of 500 and 5 microns, respectively. When expressed in wall units, these dimensions are believed to allow (Willmarth and Sharma 1984) a spatial resolution sufficient to resolve the near-wall turbulent structures. It must be said that this hot wire is too long to allow an accurate measurement of the spanwise distribution of any quantity near to the riblet wall; however, measurement locations are quite far from the close vicinity of the surface, and in fact spanwise effects are found to be absent.

The VKI constant temperature anemometer is operated at an overheat ratio of 1.4, while a continuous monitoring of the temperature in the laboratory assures that temperature variation is below 0.3° for the duration of each test.

The VKI Medium Speed Data Acquisition System is used for recording the data on the hard disk of a VAX 3300 computer. The output signal from the anemometer enters a bucking amplifier, which subtracts a fixed voltage and amplifies the remaining signal, prior to being acquired and written on disk for further analysis.

For the calibration of the hot wire, a Validyne variable inductance low full-scale range pressure transducer is used.

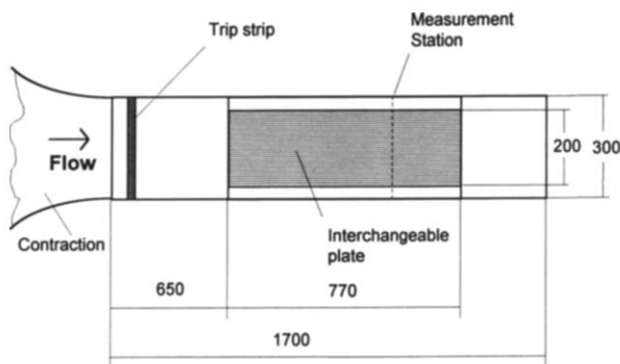


Figure 1 Sketch of the test section layout

Notation

- h Riblet height
- H Shape factor
- h_p Protrusion height
- k Threshold for VITA technique
- R Triple correlation
- s Riblet spacing
- T Time window for VITA technique
- u_τ Friction velocity
- U_{ext} Free-stream velocity

Greek symbols

- θ Momentum thickness

Superscripts

- + Non-dimensionalisation with wall variables u_τ and v

Subscripts

- c Relative to cross-flow
- 1 Relative to longitudinal flow

Experimental procedures

In the calibration phase, the hot-wire sensor is placed in the free stream near a Pitot-static tube. The resulting pressure difference at each velocity is measured by the pressure transducer and is used to obtain the free-stream velocity. The hot wire is always calibrated in the free stream of the wind tunnel just prior to starting measurements. The calibration is carried out at approximately 10 values of the velocity of the wind tunnel ranging from 0 to 6.5 m/s. The minimum free-stream velocity is approximately 0.7 m/s, so a viscous correction for the Pitot reading has been considered necessary. On the other hand, the use of a least-squares fit based on a polynomial of fourth degree for the anemometer's signal versus velocity has avoided the well-known problems encountered when using King's law at low velocities. After each single test, the probe is returned to the free stream and the calibration checked: if a significant drift has occurred, the test is repeated.

The correct positioning of the wire relative to the direction of the flow is checked by means of a theodolite. With the same instrument, thanks to an accurate lighting of the probe with a photographic spot, the position of the flat wall relative to the wire is determined within, say, 0.01 mm accuracy. The same degree of accuracy can be gained over the ribletted surface, even in the absence of the reflected image of the wire, when a black background is put after the wire. An accurate determination of the relative location of the wall has been revealed to be crucial for the computation of the friction velocity with wall-similarity methods.

Velocity signals are sampled at a sampling rate of 6250 Hz (approximately $t^+ = 0.8$) for a duration of 30 seconds. The sensitivity of the conditional technique to the frequency of acquisition and to the duration of the sampling time interval is checked, in order to avoid undesired dependence of the results on these test parameters. The analysis of data sampled at twice the frequency or for twice the acquisition time indicates no changes for both mean and instantaneous data values.

The parameters of the flat-plate turbulent boundary layer at the measurement station, located 1150 mm downstream the trip strip, are the following: free-stream velocity $U_{ext} = 5.7$ m/s; Reynolds number based on momentum thickness $Re_\theta = 1150$; shape factor $H = 1.42$. The friction velocity u_τ is determined for both surfaces by means of a least-squares fit of the slope of the nondimensional logarithmic velocity profile: this method has the advantage of the intercept of the law of the wall curve not being required; the only assumption underlying this method is that the Von Kármán constant is supposed to be unchanged for flat and riblet flows.

Longitudinal velocity profiles

The main problem to face with when dealing with velocity profiles over ribletted surfaces is that they do not have a predefined origin for the coordinate normal to the wall. However, the effect of the interaction between the riblets and the viscous sublayer of a turbulent boundary layer on the longitudinal velocity profile has been analyzed by Bechert et al. (1986) and Baron et al. (1989) by means of purely viscous calculations. This interaction can be simply considered as a shift of the origin of the profile from the peaks of the riblets of a quantity they called protrusion height (Figure 3). Even if recent studies (Bechert et al. 1990; Luchini, Manzo, and Pozzi 1991; Baron, Quadrio, and Vigevano 1991) underlined the importance of the protrusion height h_{pc} associated with the cross-flow, the use of h_{pi} for determining the virtual origin of the longitudinal velocity profiles seems to be reasonable.

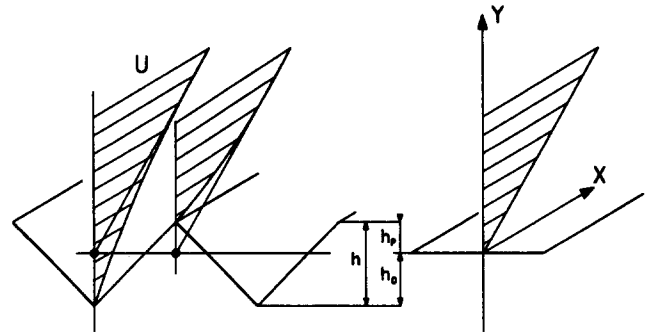


Figure 3 Definition of the protrusion height for the riblet plate

However, a recent and accurate experimental work (Choi 1989) seems to show that this hypothesis is not completely correct, because the shift indicated by h_{pi} is somewhat overestimated. In the author's opinion, this is due to the fact that the usual analytic methods for the computation of h_{pi} are based on the "ideal" geometry, while the actual geometry may be substantially different due to inaccuracies in the manufacturing process.

In the present work, the origin of the longitudinal velocity profile is considered to be located at a distance normal to the wall and equal to the height of the peaks of the ribs minus the shift expressed by h_{pi} , but the method highlighted in Baron et al. (1991) is used for the calculation of h_{pi} . This method, using conformal mapping techniques based on the Schwarz-Christoffel transformation, allows us to take into account the actual shape of the riblet contour, including possible manufacturing errors. The value of h_{pi} computed in this way gives results smaller than the h_{pi} corresponding to the ideal geometry: for the riblets shown in Figure 2, $h/s = 1$, $h_{pi} = 0.17s$ for the ideal geometry, and $h_{pi} = 0.15s$ for the real one. Therefore the calculation of h_{pi} with a method that is capable of handling the actual geometry of the riblet contour agrees with Choi's findings and allows a quantitatively correct evaluation of the influence of the riblets on the mean velocity profile.

The comparison of mean velocity profiles for flat and riblet plates in linear scales shows no difference. Logarithmic scales, on the other hand, do evidence a slight increase of u/U_{ext} over the riblet surface. The comparison of the profiles in law-of-the-wall form (Figure 4) clearly shows that, while the slope of the linear part is unchanged, the intercept of the curve

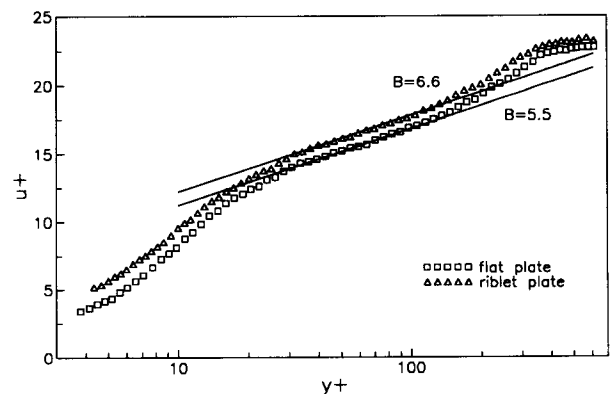
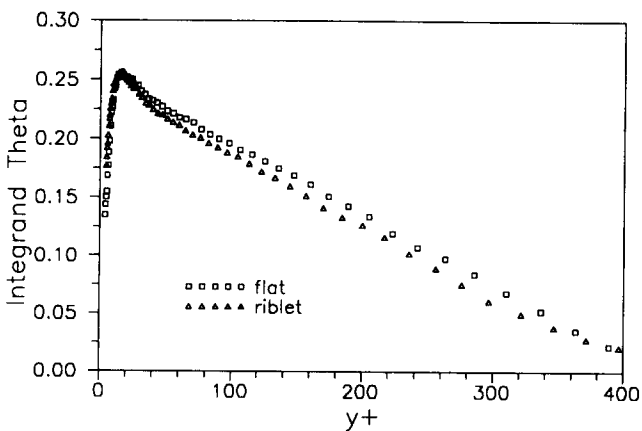


Figure 4 Law-of-the-wall plot of mean velocity profiles for flat and riblet surfaces

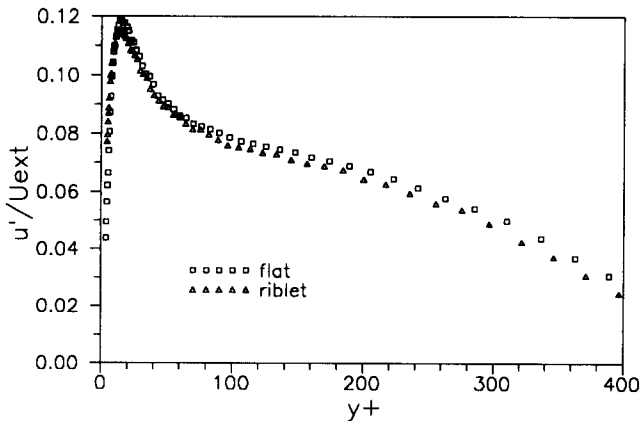
is increased from 5.5 to 6.6: this suggests that riblets could be seen as a kind of "negative roughness." This upward shift is a peculiar phenomenon for drag-reducing flows (Virk 1975) and has been also reported by Choi (1989) and Sawyer and Winter (1987). It can be considered as a change in the equilibrium condition between turbulent production and viscous dissipation in the boundary layer. An increase in viscous sublayer thickness corresponds to an increase in the dimensions of the smallest eddies in the layer, and hence to a reduction in turbulence production. For the present case, this shift corresponds to a reduction of about 3 percent in friction velocity and of 6 percent in skin-friction coefficient. This agrees with the commonly reported amount of drag reduction allowed by ribletted surfaces.

Figure 5a shows the profile of the momentum thickness integrand for both surfaces. This figure confirms the finding of Bacher and Smith (1985) and suggests that the effect of the riblets on the mean velocity profile is felt even in the logarithmic and outer regions of the boundary layer. The same evidence is put forward, for example, in the work of Squire and Savill (1987).

Root-mean-squared velocity profiles for the streamwise component of the velocity are shown in Figure 5b for flat and riblet surfaces. The commonly reported decrease for the riblet case is present, even if quite small. It is interesting to note that this reduction actually extends to a large portion of the

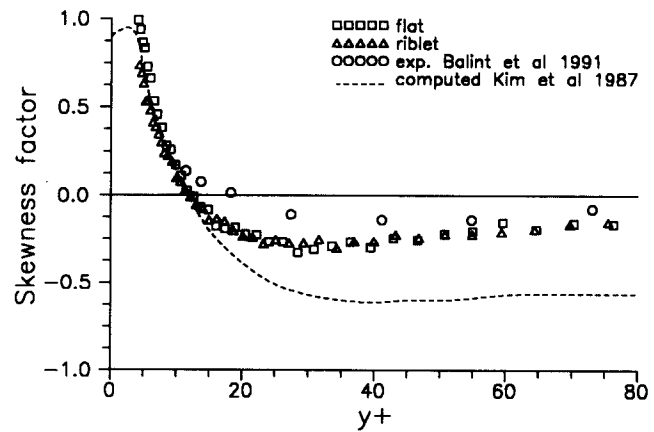


(a)

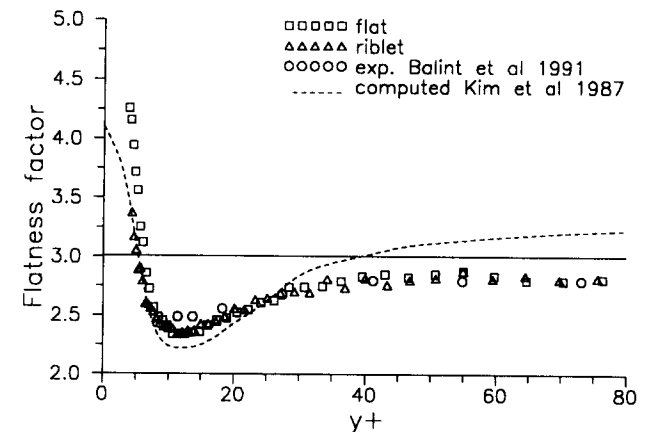


(b)

Figure 5 Integrand function for (a) θ and (b) turbulence intensity for flat and riblet surfaces



(a)



(b)

Figure 6 (a) Skewness and (b) flatness factors for flat and ribletted surfaces. Experiments from Balint et al. (1991) and computations from Kim et al. (1987) are shown for comparison

boundary layer: this is in fact a quite contradictory point, because a number of studies report on the influence of the riblets extending across the entire layer, while others measure turbulence-intensity reductions limited to the inner part of the boundary layer.

Skewness and flatness factors, shown in Figures 6a and 6b, respectively, for flat and riblet flows, are essentially unchanged. Recent experimental data from Balint et al. (1991) and from direct numerical simulation of a channel flow of Kim et al. (1987) are also shown for the flat case. The agreement is good, indicating the global reliability of the test.

Spectra and autocorrelations

Various techniques are used for the analysis of the velocity time series sampled over flat and riblet surfaces, in order to validate the test with many reliable experimental data available for the flat case. Riblet data are also shown for comparison and often do evidence some differences.

The usual velocity spectra turn out to be not very meaningful, due to the small changes induced in turbulent quantities by riblets and to the characteristic time scales of such modifications. Figure 7 shows two velocity power spectra for both surfaces, the first one (Figure 7a) corresponding to a

location in the buffer layer (14 wall units), and the second one (Figure 7b) far from the wall, at 170 wall units. While the latter exhibits no differences, in the former a slight increase in the highest frequencies and a corresponding decrease in the lower-frequency range for the riblet case is evident. This result is entirely consistent with the findings of Choi (1989), who analyzed skin-friction signals from hot-film sensors and wall-pressure fluctuations, noting for both a similar decrease for the lower frequencies over the riblet surface. Moreover, Choi notes that such reduction is evident when the skin-friction signal is analyzed, while it is just perceivable when velocity signals are examined.

The same results can be evidenced by looking at the autocorrelation function for the streamwise component of velocity. Figure 8 shows autocorrelations at approximately 14 wall units from the wall. The indication is that the duration (time/space scale) of the events seems to be lower over the riblet surface: this characteristic is present in all the autocorrelations measured in the vicinity of the wall. In contrast, no changes are evident for the outer points.

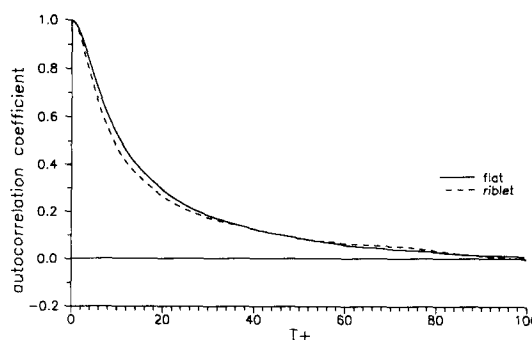


Figure 8 Autocorrelation coefficient for flat and ribletted surfaces, at $y^+ = 14$

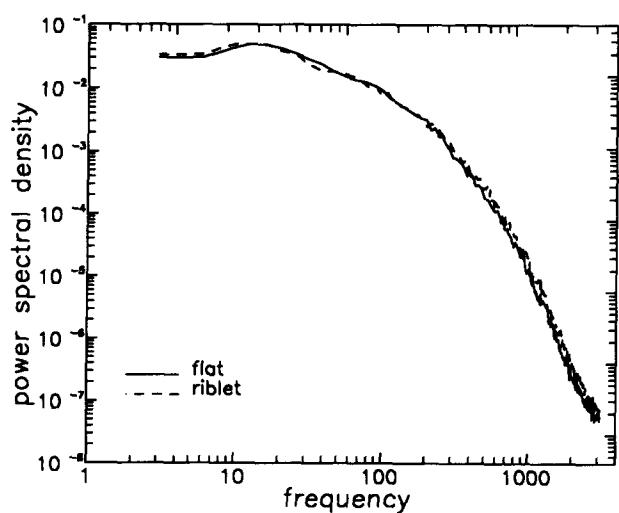
Conditional analysis

The Variable Interval Time Averaging (VITA) is probably the most widely used among the conditional techniques for the evaluation of the burst frequency. In recent years, many researchers have contributed to the development of VITA in order to gain quantitative correct information on the burst frequency. In particular, a difference has been noted (Luchick and Tiederman 1987) between ejections and bursts: VITA intrinsically detects ejections, but a variable number of ejections may be linked in the same burst. Since the single burst is the only structure somehow related to the peaks in skin friction, it therefore has a relation with the phenomenon of the drag reduction. The results presented in this chapter, based on the VITA technique, used simply as an ejection detector, are intended only as a further validation of the measurements. Nevertheless, they allow us to draw some conclusions on the instantaneous behavior of the flow over riblets.

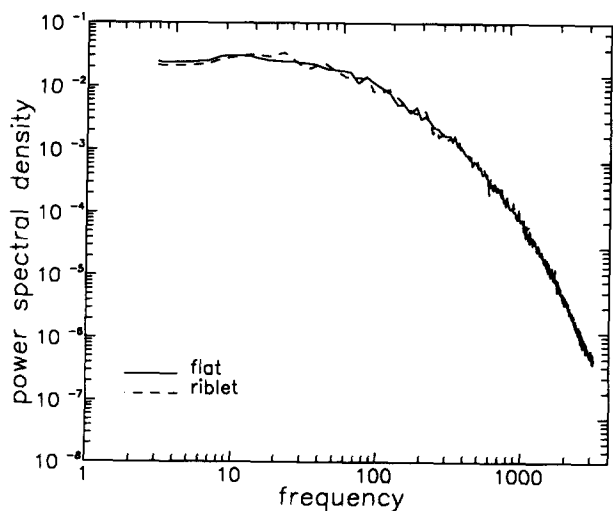
The VITA technique was developed first by Blackwelder and Kaplan (1976), to whom the reader is referred for a detailed description. Basically, VITA detects an ejection when the variance of the velocity signal over a short-time T exceeds k times the long time value, i.e., the rms of the velocity. It is then possible to add a slope criterion, so that VITA distinguishes the events where the velocity signal is increasing in the middle part of the event (ejection-related) from those with decreasing signal that are hence related to sweep-type motions. Once the events have been identified and the reference times, taken at the midpoint of the events, have been determined, a conditional (ensemble) average can be performed for the velocity pattern of the average event.

Obviously, results inferred from VITA are strongly affected by various parameters, mainly the short-time T and the threshold level k . Moreover, the problem of the choice of the variables for the nondimensionalization of the results is critical, especially when one is involved in comparing data for flat and riblet surfaces. In the literature, evidence can be found for the validity of the inner scaling, at least for low and moderate Reynolds numbers (Shah and Antonia 1989), with regard to the bursting frequency. Friction velocity, however, is always determined with some uncertainty, and this may be particularly crucial considering that it appears squared in the nondimensional frequency f^+ . For this reason, an outer scaling is preferred that, by keeping constant the Reynolds number of the test, takes advantage of the fact that the free-stream velocity is much less affected by experimental uncertainties than friction velocity is.

For the standard values $k = 1$ and $T^+ = 10$, the profile of the nondimensional ejection frequency has been computed. In Figure 9, the flat-plate data of Blackwelder and Haritonidis



(a)



(b)

Figure 7 Power spectra at (a) $y^+ = 14$ and (b) $y^+ = 170$ for flat and ribletted surfaces

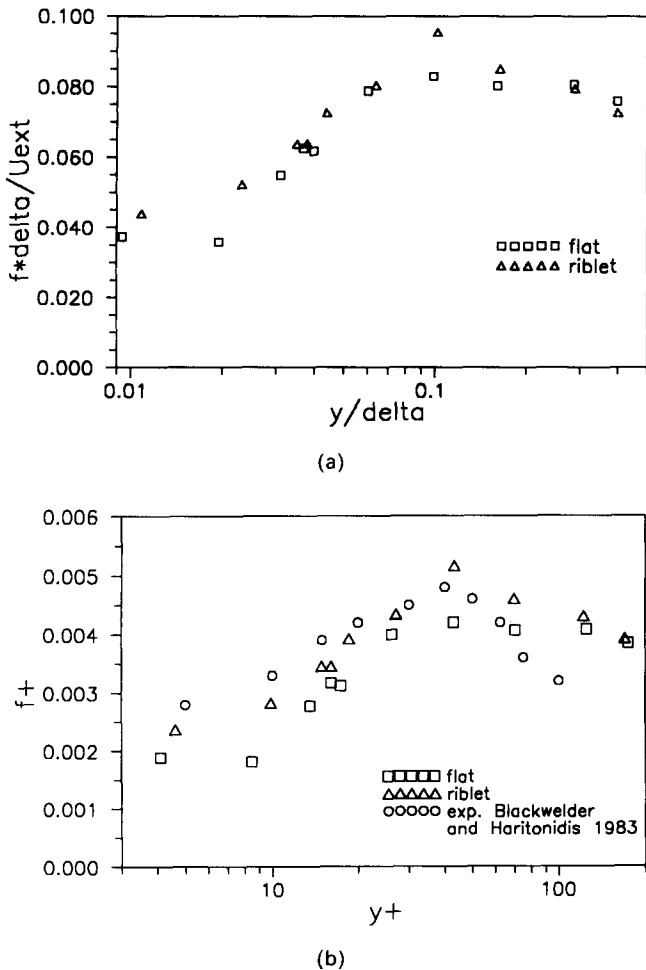


Figure 9 VITA ejection frequency with (a) outer and (b) inner scaling for flat and riblet surfaces. Experimental data from Blackwelder and Haritonidis (1983) are shown for comparison

(1983) are compared with the present measurements, using both outer (Figure 9a) and inner (Figure 9b) scaling. While the agreement with the flat-plate data is good, there is evidence for a slight increase of the frequency of the ejections over the riblet surface. This finding gives support to the results of Choi (1989) and Hoosmand et al. (1983). Walsh (1982) and Bacher and Smith (1985), on the other hand, report no changes, while Savill (1987), on the basis of visual observations, notices a 20–30 percent reduction. In fact, evaluation of the ejection frequency in comparative form is quite a difficult task; sometimes in the literature the difference between the single ejection and a whole burst is forgotten. To the knowledge of the present authors, only the work of Schwarz-van Manem et al. (1990) does in fact distinguish correctly between ejections and bursts when comparing flat and riblet flows, and reports an actual decrease of the burst frequency over riblets, supporting the hypothesis that the bursting process is less vigorous near the riblet wall. Most authors, on the other hand, report ejection frequencies increased over riblets, and this is the case even for the present test.

It is worthwhile to note, for both surfaces, the wiggle in the dimensionless frequency distribution at a distance from the wall of approximately 20–25 wall units; a particular behavior for the bursting frequency has also been observed at approximately the same distance from the wall by Schwarz-van Manem et al. (1987). We suggest that a relation may exist between this particular location and some of the coherent structures that

are typical of turbulent boundary layers and channel flows. For example, this location can be thought of as the position of the center of the streamwise vortex introduced by Kim et al. (1987), on the basis of the observation of the computed profile for the rms streamwise vorticity near the wall. They argued that this vortex, on average, has its center located at approximately 20 wall units from the wall and has a radius of 15 wall units. In a later work, Robinson (1990) visually analyzed a database generated by direct numerical simulation of a turbulent boundary layer, concluding that quasi-streamwise vortices are a dominant feature of the near-wall region, with centers located at a rather wide range of distances from the wall, with a most probable value of 20–40 wall units and a most probable diameter of 20–30 wall units. On the other hand, it appears to be hard to explain exactly the wiggle in the ejection frequency profile based on single-component hot-wire measurements and the VITA technique. More refined experimental and conditional techniques are probably needed to clarify this point further.

Figure 10 shows a typical velocity pattern obtained by conditionally averaging the VITA detections of a number of ejections. This procedure has been demonstrated to correspond to a phase alignment of the events centered on their trailing edge (Bogard and Tiederman 1987) and emphasizes the strong internal shear layer following a burst. A shorter duration and a slightly smaller amplitude is evident for the riblet case.

Figure 11a presents the behavior of the VITA ejection frequency, for smooth and riblet cases, as a function of the short-time T , at a distance of approximately 14 wall units from the wall, with the threshold fixed at a value of $k = 1$. Data for the smooth surface from Shah and Antonia (1989) are also reported, and the agreement can be considered satisfactory, since the Reynolds number is not exactly the same and since this frequency depends strongly on the Reynolds number. The results, plotted with both inner and outer scaling, show no substantial differences. There is evidence that shorter events are more frequent over the ribletted surface: this agrees with the general observation of reduced time scales of the events over the riblet surface. The duration of the averaging time T^+ at which the number of ejections over the flat wall is maximized is approximately $T^+ = 25-30$. This agrees with the value of 26 used by Bogard and Tiedermann (1987), who calibrated VITA in a way such as to detect the same number of events as flow visualization indicated. This time is somewhat shorter for the flow over riblets, and this gives further support to the indication of reduced time/space scales for this flow.

Figure 11b presents, for the same location normal to the wall, the behavior of the VITA ejection frequency for smooth and riblet cases as a function of the threshold value k , with the short-time T fixed at a value of $T^+ = 10$. Not only is the

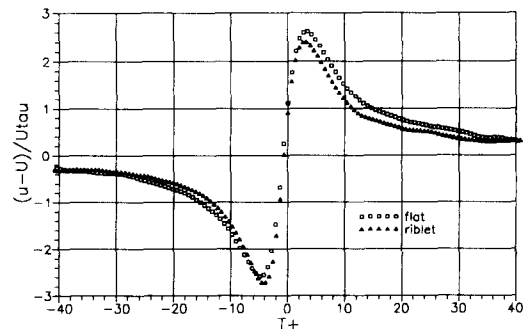


Figure 10 Conditionally averaged ejection signature over flat and riblet surfaces, at $y^+ = 14$

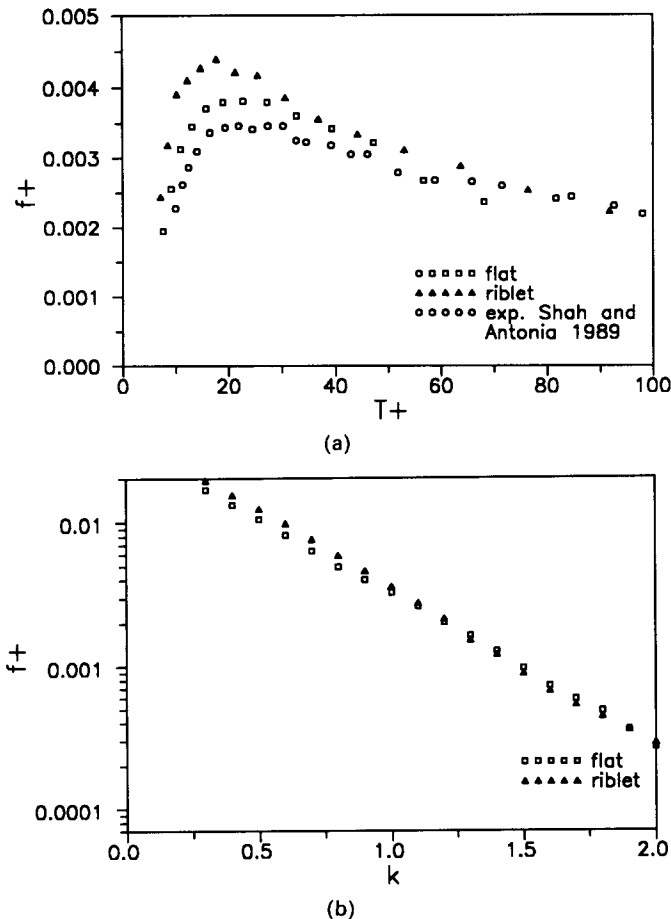


Figure 11 Dependence of VITA ejection frequency on (a) short-time T and (b) threshold level k for flat and riblet surfaces, at $y^+ = 14$. Experimental data from Shah and Antonia (1989) are shown in (a) for comparison

exponential dependence of f on k , first noted by Alfredsson and Johansson (1984) for the flat case, confirmed, but also the same trend is evident even for the riblet surface. The figure shows a common feature for the data from the buffer layer, i.e., the tendency for the riblet-plate ejection frequency to be higher for low values of k and lower for high values of k , with respect to the flat-plate ejection frequency.

Discussion and conclusions

Experimental hot-wire measurements in turbulent boundary layers over flat and ribletted walls are presented and validated by comparing present results with other experimental data available in the literature. The overall agreement of the present data with the available results is good, in terms both of mean quantities and conditional analyses.

The experimental data also allow us to ascertain some of the modifications of the flow produced by longitudinal ribs. The mean velocity profile over riblets exhibits an upward shift when plotted in the law-of-the-wall form, which is a well-known characteristic of drag-reducing flows and corresponds to an increase in thickness of the viscous sublayer. The amount of this shift is very similar to that reported by Choi (1989), provided that the actual geometry of the riblet contour is used for computing the protrusion height of the riblet surface, in order to define the virtual origin for the mean velocity profile. Turbulence intensity for the streamwise component of the

velocity is slightly reduced throughout the boundary layer, while skewness and flatness factors are unchanged.

Time series of velocity samples are analyzed by means of frequency analysis and autocorrelations. While the former seems to suggest, for the riblet flow, a small increase in the high-frequency range of the power spectrum and a corresponding decrease in the low-frequency range, autocorrelations indicate that the events are shorter over the riblet wall. Conditional averages based on the VITA technique actually confirm this reduction in time/space scales for the riblet case. Work is currently in progress for obtaining more exhaustive information on the global bursting process, using conditional techniques more sophisticated than VITA, which is known not to be best suited for the detection of the near-wall turbulent events. On the other hand, a number of studies of turbulent boundary layers and channel flows have been conducted with VITA, so this technique has been preferred here for purposes of validation of the test.

Nevertheless, the authors feel that the increase in ejection frequency as deduced from VITA and, in general, the reduction in the time/space scales of the events over the riblet surface inferred from VITA-based conditional averages and autocorrelations are consistent with the possible mechanism by which riblets do actually interact with the coherent structures that characterize a turbulent boundary layer. Such coherent structures are intrinsically three-dimensional (Johansson, Alfredsson, and Kim 1991), and hence are certainly affected by the two-dimensionality of streamwise-aligned riblets. A spatial ordering on appropriate scales may induce a more regularly arranged and fragmented phenomenology, resulting in a possible global reduction of the intensity of the bursting cycle, with a possible reduction of the occurrence of the strongest ejections. Whether or not the changes in ejection frequency and the modification of the autocorrelations for the streamwise velocity component are a direct consequence of this ordering is quite a difficult question to answer by single-point hot-wire measurements. The observation in the riblet flow of VITA ejection-frequency increase for low thresholds and decrease for higher thresholds is certainly limited by the low significance of VITA detections and by the small differences to be measured; such an observation is, however, fully consistent with the hypothesis of Schwarz-van Manem et al. (1990) of the bursting phenomenon being less vigorous in riblet flows.

The present work hence suggests that the mechanism by which riblets are effective is not only a purely viscous one: probably a direct interaction with the turbulence-producing structures of the turbulent boundary layer is also involved in their drag-reducing action.

Acknowledgments

This work has been partially supported by the Ministero dell'Università e della Ricerca Scientifica e Tecnologica. The authors wish to thank Professor M. Carbonaro and the personnel at the Von Kármán Institute for their help during the execution of the tests.

References

- Alfredsson, P. H. and Johansson, A. V. 1984. On the detection of turbulence-generating events. *J. Fluid Mech.*, **139**, 325-345
- Bacher, E. V. and Smith, C. R. 1985. A combined visualization-anemometry study of the turbulent drag reducing mechanism of triangular micro-groove surface modifications. AIAA Paper 85-0548. AIAA Shear Flow Control Conference, March 1985, Boulder, CO, USA

- Balint, J.-L., Wallace, J. M., and Vukoslavcevic, P. 1991. The velocity and vorticity vector field of a turbulent boundary layer. Part 2. Statistical properties. *J. Fluid Mech.*, **228**, 53–86
- Baron, A., Quadrio, M., and Vigevano, L. 1989. Riduzione della Resistenza di Attrito in Correnti Turbolente e Altezza di Protrusione di Pareti Scanalate. *L'Aerotecnica Missili e Spazio*, **68**, 129
- Baron, A., Quadrio, M., and Vigevano, L. 1991. On the boundary layer/riblets interaction mechanisms and the prediction of turbulent drag reduction. *Proc. XI AIDAA Conf.*, Forli, Italy
- Bechert, D. W., Bartenwerfer, M., Hoppe, G., and Reif, W.-E. 1986. Drag reduction mechanisms derived from shark skin. AIAA Publ. ICAS-86-1.8.3. XVth Congress of the International Council of Aeronautical Sciences, Sept. 1986, London
- Bechert, D. W., Bartenwerfer, M., and Hoppe, G. 1990. Turbulent drag reduction by nonplanar surfaces—A survey on the research at TU/DLR Berlin. In A. Gyr (ed.), *Structure of Turbulence and Drag Reduction*. Springer, Berlin
- Blackwelder, R. F. and Haritonidis, J. H. 1983. Scaling of the bursting frequency in turbulent boundary layers. *J. Fluid Mech.*, **76**, 87–103
- Blackwelder, R. F. and Kaplan, R. E. 1976. On the wall structure of the turbulent boundary layer. *J. Fluid Mech.*, **76**, 89–112
- Bogard, D. G. and Tiederman, W. G. 1986. Burst detection with single point velocity measurements. *J. Fluid Mech.*, **162**, 389–413
- Bogard, D. G. and Tiederman, W. G. 1987. Characteristics of ejections in turbulent channel flow. *J. Fluid Mech.*, **179**, 1–19
- Choi, K.-S. 1989. Near-wall structure of a turbulent boundary layer with riblets. *J. Fluid Mech.*, **208**, 417–458
- Coustols, E. and Cousteix, J. 1990. Experimental investigation of turbulent boundary layers manipulated with internal devices: Riblets. In A. Gyr (ed.), *Structure of Turbulence and Drag Reduction*. Springer, Berlin
- Djenidi, L., Squire, L. C., and Savill, A. M. 1991. High resolution conformal mesh computations for V, U or L groove riblets in laminar and turbulent boundary layers. In K.-S. Choi (ed.), *Recent Developments in Turbulence Management*. Kluwer, Boston
- Gallagher, J. A. and Thomas, A. S. W. 1985. Turbulent boundary layer characteristics over streamwise grooves. AIAA Paper 84-2185. AIAA 2nd Applied Aerodynamics Conference, Aug. 1984, Seattle, WA, USA
- Hoosmand, D., Youngs, R., and Wallace, J. M. 1983. An experimental study of changes in the structure of a turbulent boundary layer due to surface geometry changes. AIAA Paper 83-0230. AIAA 21st Aerospace Sciences Meeting, Jan. 1983, Reno, NV, USA
- Johansson, A. V., Alfredsson, P. H., and Kim, J. 1991. Evolution and dynamics of shear-layer structures in near-wall turbulence. *J. Fluid Mech.*, **224**, 579–599
- Kim, J., Moin, P., and Moser, R. 1987. Turbulence statistics in fully developed channel flow. *J. Fluid Mech.*, **177**, 133–166
- Lazos, B. and Wilkinson, S. P. 1988. Turbulent viscous drag reduction with thin-element riblets. *AIAA J.*, **26**(4), 496–498
- Liu, K. N., Christodoulou, C., Riccius, O., and Joseph, D. D. 1990. Drag reduction in pipes lined with riblets. *AIAA J.*, **28**(10), 1697–1698
- Luchik, T. S. and Tiederman, W. G. 1987. Timescale and structure of ejections and bursts in turbulent channel flows. *J. Fluid Mech.*, **174**, 529–552
- Luchini, P., Manzo, A., and Pozzi, A. 1991. Resistance of a grooved surface to parallel flow and cross-flow. *J. Fluid Mech.*, **228**, 87–109
- Robinson, S. K. 1990. A review of vortex structures and associated coherent motions in turbulent boundary layers. In A. Gyr (ed.), *Structure of Turbulence and Drag Reduction*. Springer, Berlin
- Rogallo, R. S. and Moin, P. 1984. Numerical simulation of turbulent flows. *Ann. Rev. Fluid Mech.*, **16**, 99–137
- Savill, A. M. 1987. Effect on turbulent boundary layer structure of longitudinal riblets alone and in combination with other devices. In L. Charnay (ed.), *Flow Visualization IV*. Hemisphere, Washington
- Sawyer, W. G. and Winter, K. G. 1987. An investigation of the effect on turbulent skin friction of surfaces with streamwise grooves. *Proc. RAS Int. Conf. on Turbulent Drag Reduction by Passive Means*, The Royal Aeronautical Society, London
- Schwarz-van Manem, A. D., Thijssen, J. H. H., Nieuwvelt, C., Krishna Prasad, K., and Nieuwstadt, F. T. M. 1990. The bursting process over drag reducing grooved surfaces. In A. Gyr (ed.), *Structure of Turbulence and Drag Reduction*. Springer, Berlin
- Shah, D. A. and Antonia, R. A. 1989. Scaling of the 'bursting' period in turbulent boundary layers and duct flows. *Phys. Fluids A*, **1**(2), 318–325
- Squire, L. C. and Savill, A. M. 1987. Some experiences of riblets at transonic speeds. *Proc. RAS Int. Conf. on Turbulent Drag Reduction by Passive Means*, The Royal Aeronautical Society, London
- Virk, P. S. 1975. Drag reduction fundamentals. *AIChEJ.*, **21**, 625
- Vukoslavcevic, P., Wallace, J. M., and Balint, J.-L. 1987. On the mechanism of viscous drag reduction using streamwise aligned riblets: a review with new results. *Proc. RAS Int. Conf. on Turbulent Drag Reduction by Passive Means*, The Royal Aeronautical Society, London
- Walsh, M. J. and Lindemann, A. M. 1984. Optimization and application of riblets for turbulent drag reduction. AIAA Paper 84-0347. AIAA 22nd Aerospace Sciences Meeting, Jan. 1984, Reno, NV, USA
- Walsh, M. J. 1982. Turbulent boundary layer drag reduction using riblets. AIAA Paper 82-0169. AIAA 20th Aerospace Sciences Meeting, Jan. 1982, Orlando, FL, USA
- Walsh, M. J. 1990. Riblets. *Prog. Astronaut. Aeronaut.*, **123**, 203–261
- Willmarth, W. W. and Sharma, L. K. 1984. Study of turbulent structures with hot wires smaller than the viscous length. *J. Fluid Mech.*, **142**, 121–149